

Case Series: Long segment extra-arachnoid fluid collections: Role of dynamic CT myelography in diagnosis and treatment planning

Shehanaz Ellika, Horia Marin, Mitchell Pace, Daniel Newman, Muwaffak Abdulhak, Maximilian Kole

Department of Radiology, Henry Ford Health System, Detroit, MI, USA

Correspondence: Dr. Horia Marin, Division of Neuroradiology, Department of Radiology, Henry Ford Health Systems, 2799 West Grand Blvd, Detroit, 48202. MI, USA. E-mail: marinh@rad.hfh.edu

Abstract

We report five patients in whom spinal MRI revealed extra-arachnoid fluid collections. These spinal fluid collections most likely resulted from accumulation of cerebrospinal fluid (CSF) from a dural leak. The patients presented with either compressive myelopathy due to the cyst or superficial siderosis (SS). All of these fluid collections were long segment, and MRI demonstrated the fluid collections but not the exact site of leak. Dynamic CT myelogram demonstrated the site of leak and helped in the management of these complicated cases. Moreover, we also found that the epicenter of the fluid collection on MRI was different from the location of the leak on a dynamic CT myelogram. Knowledge of these associations can be helpful when selecting the imaging studies to facilitate diagnosis and treatment.

Key words: Long segment; extra-arachnoid fluid collections; spine; dynamic CT myelography

Introduction

Spinal extra-arachnoid fluid collections most likely result from accumulation of cerebrospinal fluid (CSF) due to a dural leak. In most patients, the site of leak can be localized using conventional myelography with delayed CT imaging. However, in some patients with spinal CSF leaks and long spinal fluid collections, there are multiple leaks or large dural tears and the time delay during transfer between myelography and CT scan allows the extrathecal contrast to spread over multiple levels, thus making identification of their source impossible.^[1] MRI in all our cases demonstrated the spinal fluid collections but not the exact site of leak. Our

study demonstrates the utility of dynamic CT myelogram in identifying the site of leak and its role in the management of these complicated cases.

Case Reports

Case 1

A 56-year-old presented with a two-year history of progressive bilateral weakness, incoordination of the lower extremities, and progressive hearing loss. Physical examination revealed bilateral lower limb dysmetria, with exaggerated lower limb deep tendon reflexes and Babinski sign bilaterally. He had decreased vibration sensation and proprioception in the lower extremities, walked with a wide-based gait, and had a positive Romberg test. In addition, he had bilateral asymmetric high-frequency sensorineural hearing loss. Cerebrospinal fluid (CSF) and cytological analyses revealed xanthochromia and hemosiderin-laden macrophages.

Typical findings of superficial siderosis (SS) were seen in the brain [Figure 1A] and the spinal cord on MRI. There was long-segment spinal cord T2 signal abnormality, which

Access this article online

Quick Response Code:



Website:
www.ijri.org

DOI:
10.4103/0971-3026.101083

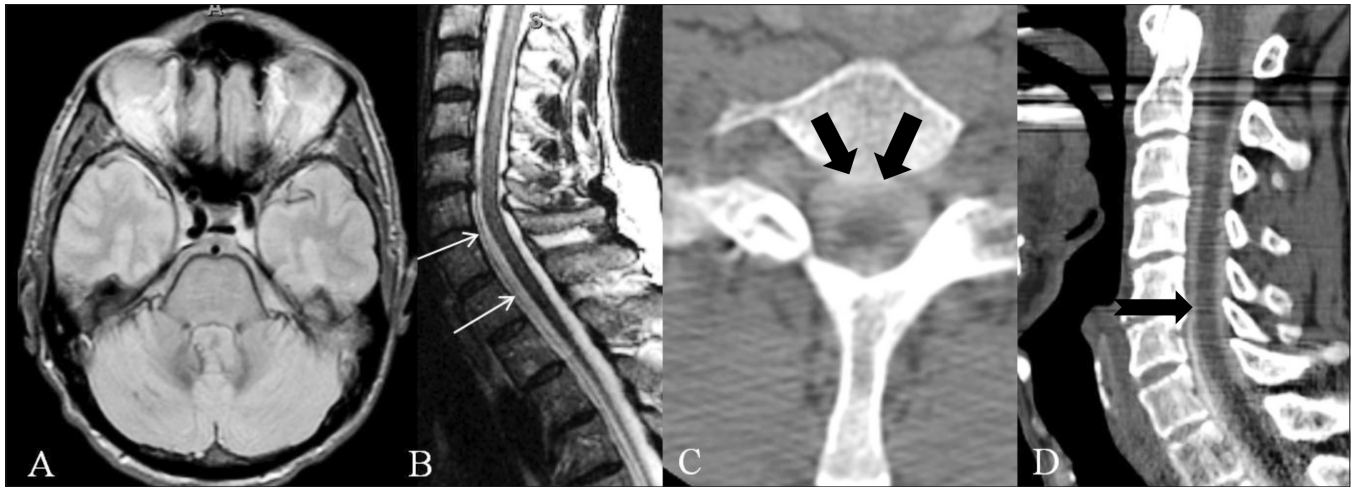


Figure 1 (A-D): Axial gradient-echo MRI (A) shows superficial siderosis around the cerebellar hemispheres and brainstem. (B) Sagittal T2W spine MRI shows a ventral fluid collection (thin white arrows) in the thoracic spine. Axial (C) and sagittal (D) immediate CT myelogram shows contrast pooling in the ventral collection (thick black arrows) with similar contrast density in the thecal sac and ventral fluid collection at the C₅-C₆ disc level, suggesting site of leak (notched black arrow)

extended from the medulla to the D₂ spinal segment, with no cord expansion [Figure 1B]. Also noted was a long-segment, nonenhancing, extra-arachnoid fluid collection along the ventral aspect of the thecal sac, extending from C₆ to the D₁₂ spinal levels, with minimal mass effect on the thecal sac [Figure 1B]. On contrast-enhanced scans there was no abnormal intramedullary enhancement, but vascular enhancement was seen along the anterior and posterior aspects of the cord and lower brainstem, in the midline. The patient subsequently underwent two brain and spine angiograms for the abnormal vascular enhancement seen on the MRI and suspicion of spinal dural arteriovenous fistula, but the investigations were normal.

Dynamic CT myelography was performed, which also showed the ventral extra arachnoid fluid collection, indicating communication between the collection and the thecal sac. There was similar contrast density in the ventral fluid collection and the thecal sac at the C₅-C₆ level on the immediate dynamic CT myelogram, suggesting site of leak [Figure 1C and D]. The patient was managed conservatively with steroids, and follow-up MRI and repeat dynamic myelography done 1 year later showed spontaneous resolution of the ventral extra arachnoid fluid collection with persistent superficial siderosis. Patient had persistent ataxia, hearing loss and myelopathy which were presumed to be due to superficial siderosis.

Case 2

A 70-year-old male reported with imbalance, ascending numbness and tingling in the lower extremities and progressive hearing loss since 1 year. Sensory exam demonstrated decreased vibration sense in the hands and feet, with decreased perception of pinprick and cold sensation below the ankle. Hoffmann and Babinski signs were present bilaterally. MRI of the brain and spine

demonstrated the typical findings of SS in the brain [Figure 2A-D] and spinal cord [Figure 2E and F]. No abnormal flow voids were noted on the brain and spine MRI to suggest an arteriovenous malformation. Also demonstrated was a nonenhancing, extra-arachnoid, ventral fluid collection extending from C₂ to D₉, causing minimal indentation of the anterior thecal sac [Figure 2E and F]. Dynamic CT myelogram was done, which identified a communication between the thecal sac and the ventral fluid collection at the D₁ level [Figure 2G and H]. At surgery, there was a communication between the ventral fluid collection and the thecal sac on the right side above the right D₁ pedicle, with multiple abnormal blood vessels in the right D₁ nerve root sleeve. One of them was potentially the source of the bleeding responsible for the SS and was surgically clipped and the CSF leak was repaired. After surgery, patient developed postoperative complications with pseudomeningocele formation which required re-exploration. After the second surgery patient had stable symptoms of superficial siderosis with improvement of upper extremity signs.

Case 3

A 58-year-old lady presented with history of a motor vehicle accident followed by a 10-year history of progressive painless wasting and weakness of the left upper extremity. On examination, there was decreased bulk in the intrinsic hand and distal forearm muscles on the left. Hoffman sign and finger flexor jerk were absent on the left. MRI of the spine showed an extra-arachnoid fluid collection extending anteriorly from C₆ to D₁ spinal level, with mild indentation of the thecal sac; the fluid was seen tracking to the left posterolateral epidural space from C₇ to the D₂ levels and becoming ventral in the upper to mid thoracic spine [Figure 3A-D]. Cord T2 signal changes were noted from C₄ to D₁ along with cord atrophy [Figure 3A-D].

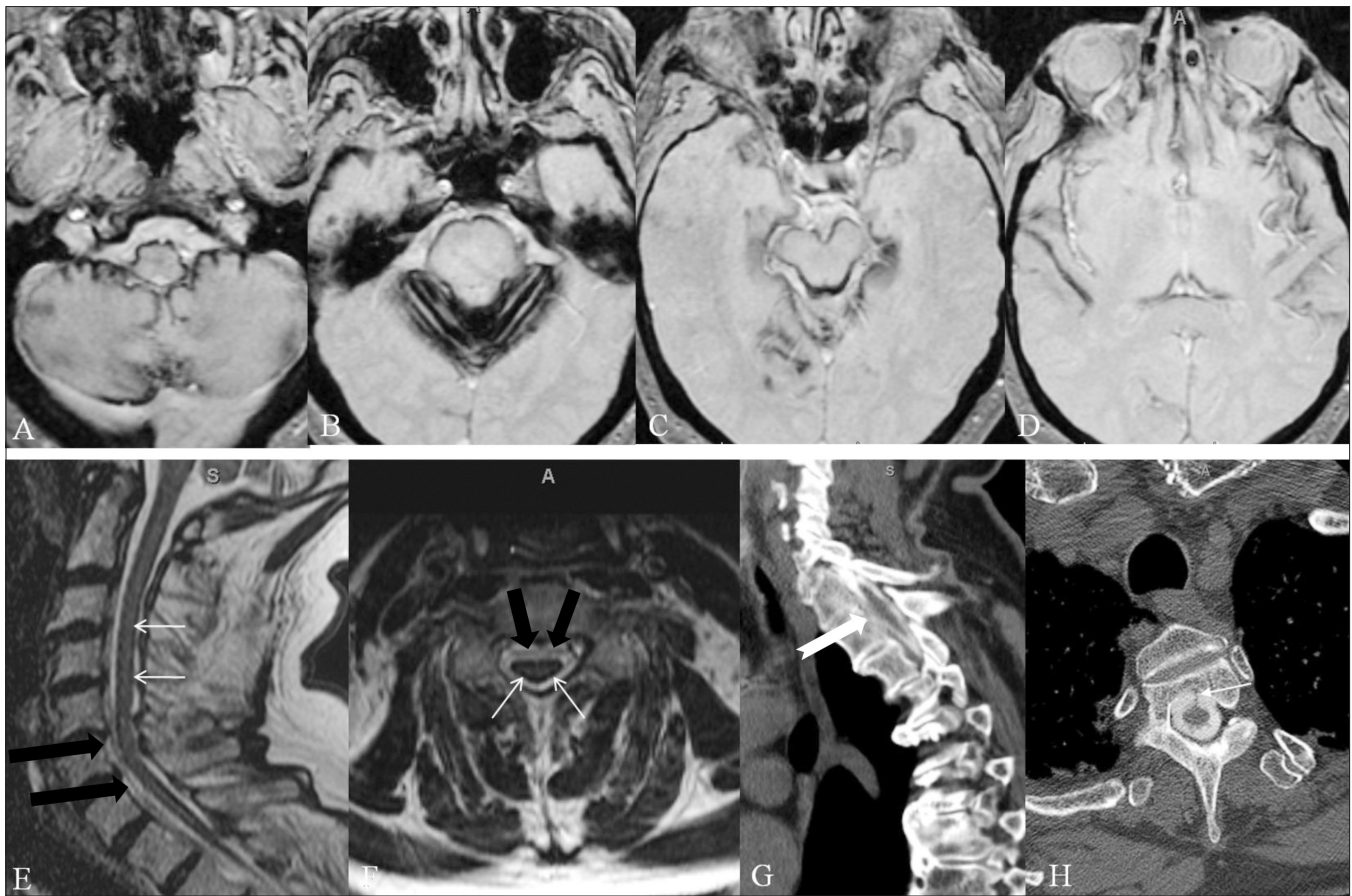


Figure 2 (A-H): Axial gradient-echo MRIs from inferior to superior (A-D) shows superficial siderosis around the cerebellar folia and brainstem. Sagittal T2W (E) and axial T2W (F) spine MRIs show a ventral fluid collection extending from C₂-D₉ (thick black arrows). Also noted is a thin rim of T2 hypointensity around the surface of the cord (thin white arrows) due to superficial siderosis. Sagittal immediate dynamic CT myelogram (G) shows leakage of contrast into the ventral collection at T₁-T₂ level (notched white arrow). Axial immediate dynamic CT myelogram (H) shows a lucent line in the ventral fluid collection, which may represent a fibrous band (thin white arrow). At surgery, a connection between the ventral collection and the main dural cavity was identified on the right at the T₁-T₂ level. Also identified were multiple abnormal blood vessels near the right nerve root sleeve, one of which was an acute bleeder and was the potential source of bleeding responsible for the superficial siderosis

A dynamic immediate CT myelogram in the left lateral decubitus showed differential opacification between the thecal sac and the collection [Figure 3E] and communication between the fluid collection and thecal sac, with asymmetric accumulation of contrast in the left C₈ perineural sheath, suggestive of a traumatic pseudomeningocele [Figure 3F]. On the delayed images there was progressively increasing accumulation of contrast within the fluid collection, with homogenous contrast opacification [Figure 3G]. Given the lack of significant cord compression, surgery was not offered to the patient.

Follow MRI showed spontaneous improvement in the size of the fluid collection with stable weakness in the left upper extremity.

Case 4

A 22-year-old man presented with history of a motor vehicle crash and was evaluated for complaints of neck pain with tingling and numbness in both the upper

extremities immediately after the crash, with progression over the next two weeks. His examination revealed brisk tendon reflexes in the upper extremities, with a positive Hoffman test bilaterally. Spinal MRI showed a long-segment, nonenhancing, ventral extra-arachnoid fluid collection extending from C₂ to L₃ [Figure 4A-D]. The thecal sac and cervical cord were displaced posteriorly by this fluid collection [Figure 4A-D]. A dynamic immediate CT myelogram showed equal contrast density in the thecal sac and the ventral fluid collection at the C₃-C₄ and C₄-C₅ levels [Figure 4E and F], suggesting the site of leak with differential opacification below the level of leak [Figure 4G and H]. In addition, there were pseudomeningoceles involving the left C₆, C₇, and C₈ nerve roots [Figure 4I-L]. A C₅-C₇ laminectomy was done and the ventral fluid collection was aspirated, followed by closure of the dura in a watertight fashion. The leak could not be identified intraoperatively. A follow-up MRI 6 months later showed persistence of the ventral fluid collections with worsening of symptoms. Patient subsequently had a second surgery

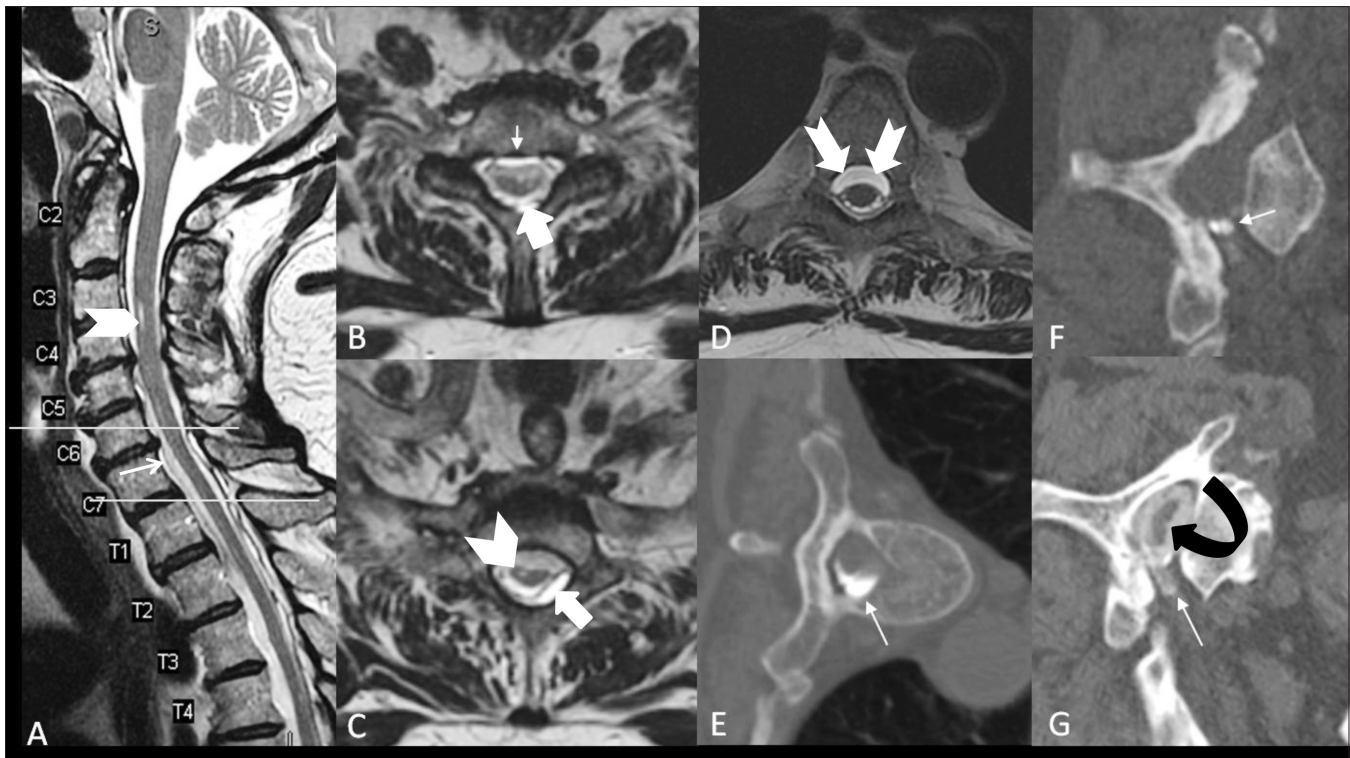


Figure 3 (A-G): Sagittal (A) and axial (B-D) T2W spine MRI showing extra-arachnoid fluid collection extending anteriorly from C₆ to T₁ level (thin white arrow), with mild indentation of the thecal sac, tracking to the left posterolateral epidural space (thick white arrow) from C₆ to T₂ level and becoming ventral in the upper thoracic spine (notched arrow). Cord T2 signal changes are also noted (arrow head) (A-C). Dynamic immediate CT myelogram (E, F) in left lateral decubitus position showed communication between the collection and thecal sac and asymmetric accumulation of contrast in the left C₆ perineural sheath (white arrow), suggestive of traumatic pseudomeningocele (F). On the delayed CT myelogram images (G) there was progressively increasing accumulation of contrast within the ventral extra arachnoid collection (curved arrow)

with placement of cysto-subarachnoid drainage catheter, which was followed by significant clinical improvement.

Case 5

A 36-year-old man presented with a 3-year history of progressive weakness of his hands-left more than right. At 19 years of age he had suffered a stab injury to the base of the neck on the right and had developed right leg weakness that had progressively improved over the next few months and returned to baseline. On examination, there was decreased bulk in the left forearm, with minimally increased tone in the right upper and right lower extremities. There was significant weakness in the left first dorsal interosseous muscles, with diminished left handgrip. He had slightly reduced vibration sense up to the level of the ankle bilaterally, slightly worse on the left side. There was bilateral sustained clonus and bilateral Hoffman sign. Spinal MRI revealed a focal area of cystic myelomalacia within the right hemicord at the D₁-D₂ level, with focal right posterolateral tethering of the cord [Figure 5A-C]. A ventral extra-arachnoid fluid collection was seen extending from C₅ through L₂ levels [Figure 5A-C]. Dynamic immediate CT myelogram demonstrated a small area of triangular contrast extravasation along the right posterolateral aspect of the thecal sac at the D₁-D₂ level and an unopacified ventral

fluid collection [Figure 5D-F]). Delayed CT myelogram showed a left posterolateral fluid collection, with differential opacification of the thoracic ventral fluid collection [Figure 5G-J]. At surgery, the right posterolateral leak was identified and repaired. Follow up MRI demonstrated stable ventral fluid collections with clinical improvement of the left upper extremity weakness.

Discussion

Spinal extra-arachnoid fluid collections are CSF-filled cavities located within the spinal canal and outside the thecal sac. These fluid-filled cavities have been variably referred to as meningoceles, pseudomeningoceles, diverticula, epidural cyst, or simply as 'fluid collections.'^[2] These spinal extra-arachnoid fluid collections are caused by extradural CSF leaks which can be spontaneous, caused by traumatic or iatrogenic (during surgery) dural injury or traumatic avulsion of the brachial plexus.^[3-7] This theory is supported by the observed communication between the extradural spinal collection and the thecal sac seen at dynamic CT myelography in our patients and also noted by several authors.^[7-10] Differential diagnosis for these spinal collections include extradural arachnoid cysts.

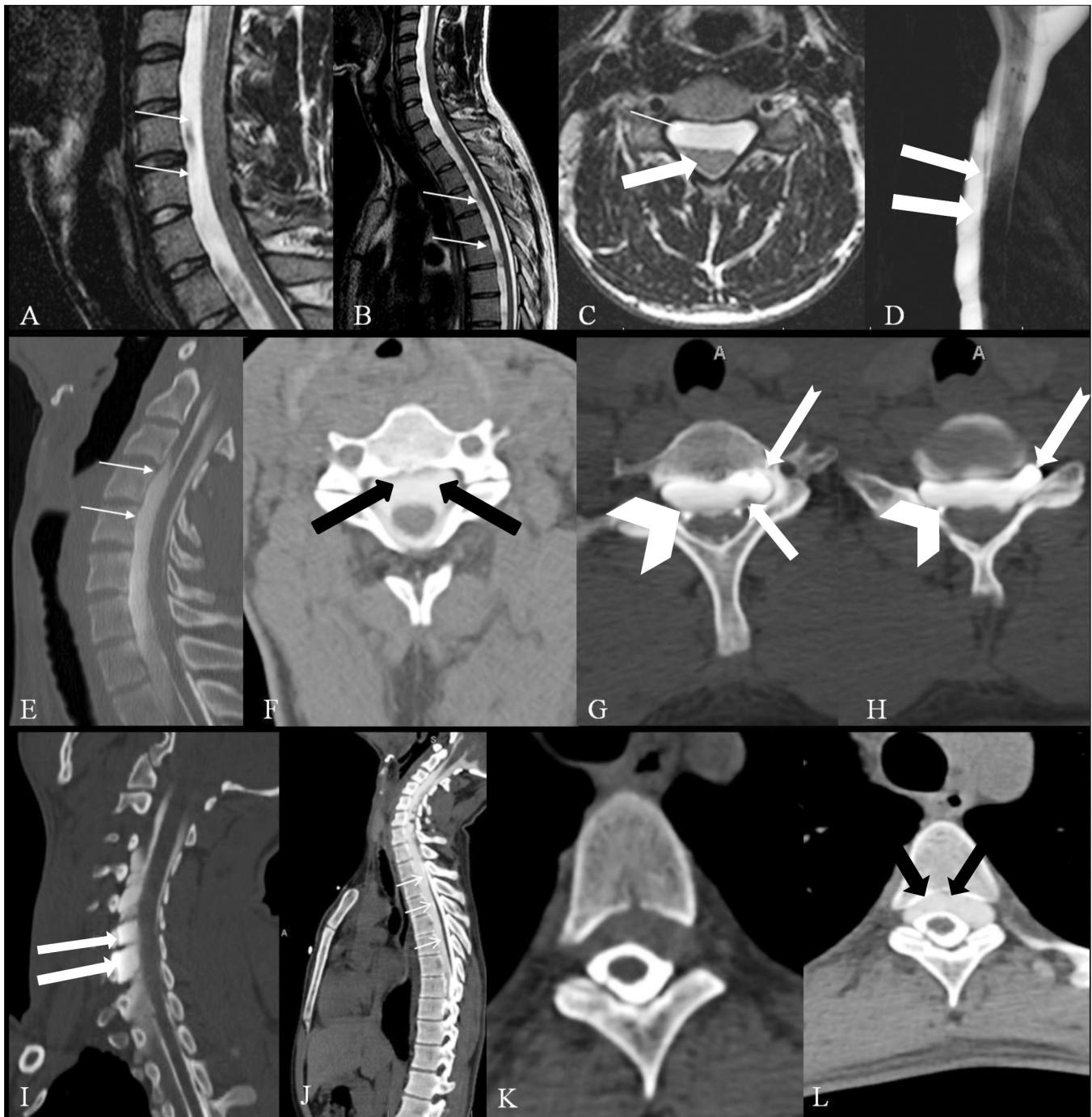


Figure 4 (A-L): Sagittal T2 W (A,B) and axial T2W (C) spine MRIs show the ventral extra-arachnoid fluid collection (thin white arrows) extending from C₂ down to L₃ level. The thecal sac and cervical cord is displaced posteriorly by this fluid collection (thick white arrow). MR myelogram (D) also demonstrates the ventral fluid collection (thick white arrows). Sagittal immediate dynamic CT myelogram (E) shows opacification of the ventral fluid collection, with similar density of contrast in ventral fluid collection and the thecal sac at C₃-C₄ and C₄-C₅ disc levels (white arrows). Axial immediate dynamic CT myelogram at C₄-C₅ (F) disc level shows contrast density in the thecal sac and the ventral fluid collection to be similar (thick black arrows), suggesting site of leak. Axial immediate dynamic CT myelogram at C₆-C₇ (G) disc level shows differential opacification of the ventral fluid collection and the thecal sac (thick white arrows). In addition, pseudomeningoceles were identified on the left at multiple levels, more prominent at C₆-C₇ (G) and C₇-T₁ (H) levels (notched arrows). The nerve root sleeves on the right appear to be separated from the collection, with the differential contrast opacity within the right-sided nerve root sleeves (arrowheads); however, the left-sided nerve root sleeves (thick white arrow) appear to be incorporated within the ventral fluid collection. Also, note the effacement of the CSF space surrounding the cord due to extrinsic compression by the ventral fluid collection (G and H). The epicenter of the compression (C₆-C₇) is lower than the site of leak (C₄-C₅). Sagittal oblique reconstructions (I) of early dynamic CT myelogram shows pseudomeningoceles at multiple levels (white arrows) on the left in the cervical spine. Sagittal delayed dynamic CT myelogram (J) shows inferior extension of the ventral fluid collection into the thoracic region (white arrows). Axial immediate (K) and axial delayed (L) images from dynamic CT myelogram of the thoracic spine show progressive equilibration of contrast in the ventral fluid collection in the thoracic region on the delayed scans (L) (thick black arrows)

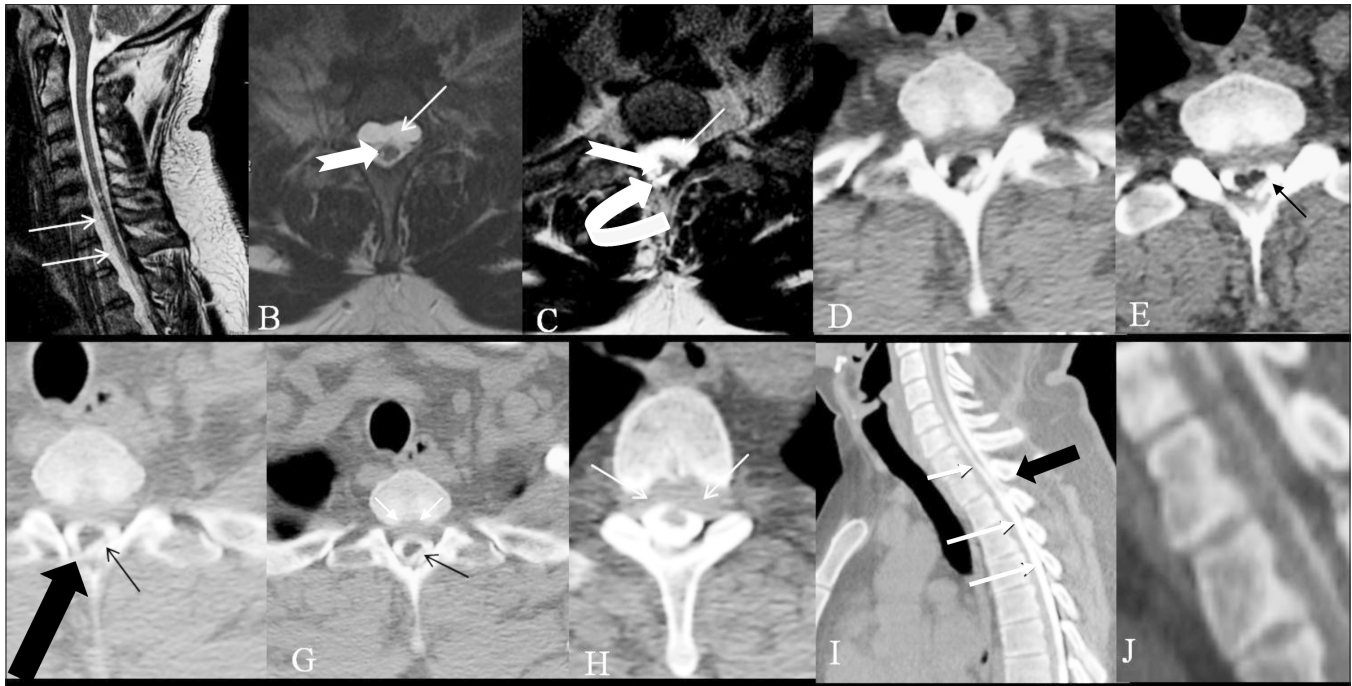


Figure 5 (A-J): Sagittal (A) and axial T2W (B) cervical spinal MRIs demonstrate ventral extradural fluid collection (white arrows) and focal myelomalacia involving the right side of the cord (notched arrow) at the site of the stab injury. Axial T2W images at T1–T2 disc level (C) again demonstrate the ventral fluid collection and the cystic myelomalacia in the right hemicord, with focal right posterolateral tethering of the cord (curved arrow). Serial axial images obtained immediately after lateral decubitus (D), after 1×360° rotation (E), and after 2×360° rotations (F) show right posterolateral leak of contrast (thick black arrows) and left posterolateral fluid collection (E,F) (black arrow). Delayed axial CT myelogram (G,H) show differential opacification of the thoracic ventral fluid collection (white arrows). Sagittal delayed dynamic CT myelogram (I) demonstrates small triangular contrast extravasation posterior to the thecal sac (blue arrows) and differential opacification of the ventral fluid collection (white arrows). Oblique sagittal delayed CT myelogram reformats (J) show contrast leak (thick black arrow)

Spinal extra-arachnoid fluid collections may present with symptoms related to compressive myelopathy from the collection, SS, or intracranial hypotension. The pathogenesis is usually considered to be an occult CSF leak through small defects in the meninges. Pulsatile CSF dynamics,^[11] presence of an osmotic gradient between the subarachnoid space and cyst,^[12] and valve-like mechanism between the fluid collection and subarachnoid space^[13] may play important roles in the enlargement of these spinal extra-arachnoid fluid collections, which can then cause cord compression and cord signal changes.

In patients with spinal fluid collections, it essential to not only demonstrate the leak but also the site and morphology, because treatment strategy differs dependent on these characteristics. The goal of imaging is to diagnose the extra-arachnoid fluid collections and pseudomeningoceles and also, specifically, to identify the dural defect; this is best characterized by MRI, MR myelography CT myelography, and digital subtraction myelography.^[2,14-16]

All our cases demonstrated long-segment nonenhancing extra-arachnoid spinal fluid collections that were isointense to CSF on T1W and T2W images. Spinal MRI demonstrated the spinal fluid collections but did not demonstrate the

actual site of CSF leak.

In most patients, the site of leak can be localized by using conventional myelography, with delayed CT scans for slower leaks. However, when there are multiple leaks or large dural tears, the time delay during transfer between the myelographic portion of the examination and CT scan allows the extrathecal contrast to spread over multiple levels, thus limiting the ability to localize the leaks.^[1] The exact site of dural defect in intraspinal collections spanning long segments can be accurately localized with dynamic CT myelography,^[16,17] which was first introduced for localizing high-flow CSF leaks.^[1]

The technique of dynamic CT myelography involves CT acquisition during the initial introduction of the myelographic contrast media into the thecal sac. Specifically, our technique involves puncturing the thecal sac in the lumbar region on the CT Table with the patient in the prone position. A short-segment CT scan over the lumbar segments confirms accurate intrathecal positioning of the needle (scanning the entire spine before injection of contrast is usually not necessary and also increases the radiation dose of the examination). After injection of 10-15 ml of myelographic contrast media, the patient is mobilized to

displace the contrast into the spinal segment of interest, e.g., by having the patient adopt a Trendelenburg position to displace the contrast column into the thoracic and cervical spine. The immediate CT acquisition is obtained with the collection in the dependent position. A second delayed acquisition can be obtained after asking the patient to rotate 360°.

Dynamic CT myelogram in all of our cases showed contrast opacification of the extra-arachnoid fluid collection, confirming free communication with the subarachnoid space. Early dynamic CT myelography demonstrated the site of leak where there was similar contrast density within the thecal sac and the fluid collections. All patients had long-segment extra-arachnoid fluid collections, with the epicenter of the collection at a site different from the site of the dural leak.

We understand that dynamic CT myelography is more invasive, has higher radiation dose and is more time intensive. We thus, do not advocate routine use of this technique for all patients with spinal fluid collections.^[1] We reserve this technique for a subset of patients with long segment spinal fluid collections with presumed high-flow spinal CSF leaks.

Spinal extra-arachnoid pseudomeningoceles are rare and can be an unrecognized source of chronic bleeding into the subarachnoid space, leading to SS.^[18] SS occurs due to chronic or repeated slow hemorrhage into the subarachnoid space that leads to hemosiderin deposition over the cerebral and spinal leptomeninges.^[19] Etiologies for SS include root avulsions, tumors, vascular malformations, and brain or spine surgery.^[20] In a 1995 survey of the reported SS cases in the literature, a dural pathology was found in 47% of cases.^[20] This included CSF cavity lesions (e.g., meningoceles, pseudomeningoceles, pseudoencephaloceles, cavity remaining after a hemispherectomy, and chronic suboccipital hematomas), or root pathology (e.g., root avulsions or epidural cysts).^[20] Brachial plexus injury with associated nerve root avulsion is also a common association.^[17,21-24]

The association of a spinal fluid collection that communicates with the subarachnoid space in patients with SS and history of trauma has been recently been recognized by Kumar *et al.*,^[16] and the authors stress the importance of looking for such a communication using dynamic CT-myelogram. In our series, two patients presented with SS, and in one of them extensive brain and spine angiograms did not reveal spinal arteriovenous malformations. It is important to remember that in patients with SS with long-segment extra-arachnoid fluid collections, the bleeding source is usually in the spine, and dynamic CT myelogram helps to locate the exact site of the leak, which then helps in surgical planning.

Conclusions

Our cases illustrate a complex, poorly understood, and difficult-to-clinically-manage entity, which on imaging is represented by extra-arachnoid fluid collections related to occult dural tear and CSF leak. The exact location of the leak is best identified using dynamic CT myelography, and accurate localization helps in planning surgical treatment.

References

1. Luetmer PH, Mokri B. Dynamic CT myelography: A technique for localizing high-flow spinal cerebrospinal fluid leaks. *AJNR Am J Neuroradiol* 2003;24:1711-4.
2. Kumar N. Neuroimaging in superficial siderosis: An in-depth look. *AJNR Am J Neuroradiol* 2010;31:5-14.
3. Burres KP, Conley FK. Progressive neurological dysfunction secondary to postoperative cervical pseudomeningocele in a C-4 quadriplegic. Case report. *J Neurosurg* 1978;48:289-91.
4. Kachooie A, Bloch R, Banna M. Post-traumatic dorsal pseudomeningocele. *J Can Assoc Radiol* 1985;36:262-3.
5. Miravet E, Sinisterra S, Birchansky S, Papazian O, Tuite G, Grossman JA, *et al.* Cervicothoracic extradural arachnoid cyst: Possible association with obstetric brachial plexus palsy. *J Child Neurol* 2002;17:770-2.
6. Pal HK, Bhatti GB, Deb S, Mishra S. Traumatic pseudomeningocele at cranio-vertebral junction following stab injury. *Injury* 1998;29:142-3.
7. Rabin BM, Roychowdhury S, Meyer JR, Cohen BA, LaPat KD, Russell EJ. Spontaneous intracranial hypotension: spinal MR findings. *AJNR Am J Neuroradiol* 1998;19:1034-9.
8. Fishman RA, Dillon WP. Dural enhancement and cerebral displacement secondary to intracranial hypotension. *Neurology* 1993;43:609-11.
9. Rando TA, Fishman RA. Spontaneous intracranial hypotension: Report of two cases and review of the literature. *Neurology* 1992;42:481-7.
10. Schievink W. Spontaneous spinal cerebrospinal fluid leaks and intracranial hypotension. *JAMA* 2006;295:2286-96.
11. McCrum C, Williams B. Spinal extradural arachnoid pouches. Report of two cases. *J Neurosurg* 1982;57:849-52.
12. Lake PA, Minckler J, Scanlan RL. Spinal epidural cyst: Theories of pathogenesis. Case report. *J Neurosurg* 1974;40:774-8.
13. Nabors MW, Pait TG, Byrd EB, Karim NO, Davis DO, Kobrine AI, *et al.* Updated assessment and current classification of spinal meningeal cysts. *J Neurosurg* 1988;68:366-77.
14. Holle D, Sandalcioglu IE, Gizewski ER, Asgari S, Timmann D, Diener HC, *et al.* Association of superficial siderosis of the central nervous system and low pressure headache. *J Neurol* 2008;255:1081-2.
15. Hoxworth JM, Patel AC, Bosch EP, Nelson KD. Localization of a rapid CSF leak with digital subtraction myelography. *AJNR Am J Neuroradiol* 2009;30:516-9.
16. Kumar N, Lindell EP, Wilden JA, Davis DH. Role of dynamic CT myelography in identifying the etiology of superficial siderosis. *Neurology* 2005;65:486-8.
17. Kumar N, Cohen-Gadol AA, Wright RA, Miller GM, Piepgras DG, Ahlskog JE. Superficial siderosis. *Neurology* 2006;66:1144-52.
18. Kole MK, Steven D, Kirk A, Lownie SP. Superficial siderosis of the central nervous system from a bleeding pseudomeningocele. Case illustration. *J Neurosurg* 2004;100:718.

19. Gomori JM, Grossman RI, Bilaniuk LT, Zimmerman RA, Goldberg HI. High-field MR imaging of superficial siderosis of the central nervous system. *J Comput Assist Tomogr* 1985;9:972-5.
20. Fearnley JM, Stevens JM, Rudge P. Superficial siderosis of the central nervous system. *Brain* 1995;118:1051-66.
21. Bonito V, Agostinis C, Ferraresi S, Defanti CA. Superficial siderosis of the central nervous system after brachial plexus injury. Case report. *J Neurosurg* 1994;80:931-4.
22. Cohen-Gadol AA, Krauss WE, Spinner RJ. Delayed central nervous system superficial siderosis following brachial plexus avulsion injury. Report of three cases. *Neurosurg Focus* 2004;16:E10.
23. Konitsiotis S, Argyropoulou MI, Kosta P, Giannopoulou M, Efremidis SC, Kyritsis AP. CNS siderosis after brachial plexus avulsion. *Neurology* 2002;58:505.
24. Tapscott SJ, Eskridge J, Kliot M. Surgical management of superficial siderosis following cervical nerve root avulsion. *Ann Neurol* 1996;40:936-40.

Cite this article as: Ellika S, Marin H, Pace M, Newman D, Abdulhak M, Kole M. Case Series: Long segment extra-arachnoid fluid collections: Role of dynamic CT myelography in diagnosis and treatment planning. *Indian J Radiol Imaging* 2012;22:108-15.

Source of Support: Nil, **Conflict of Interest:** None declared.

Author Help: Online submission of the manuscripts

Articles can be submitted online from <http://www.journalonweb.com>. For online submission, the articles should be prepared in two files (first page file and article file). Images should be submitted separately.

1) **First Page File:**

Prepare the title page, covering letter, acknowledgement etc. using a word processor program. All information related to your identity should be included here. Use text/rtf/doc/pdf files. Do not zip the files.

2) **Article File:**

The main text of the article, beginning with the Abstract to References (including tables) should be in this file. Do not include any information (such as acknowledgement, your names in page headers etc.) in this file. Use text/rtf/doc/pdf files. Do not zip the files. Limit the file size to 1024 kb. Do not incorporate images in the file. If file size is large, graphs can be submitted separately as images, without their being incorporated in the article file. This will reduce the size of the file.

3) **Images:**

Submit good quality color images. Each image should be less than **4096 kb (4 MB)** in size. The size of the image can be reduced by decreasing the actual height and width of the images (keep up to about 6 inches and up to about 1800 x 1200 pixels). JPEG is the most suitable file format. The image quality should be good enough to judge the scientific value of the image. For the purpose of printing, always retain a good quality, high resolution image. This high resolution image should be sent to the editorial office at the time of sending a revised article.

4) **Legends:**

Legends for the figures/images should be included at the end of the article file.